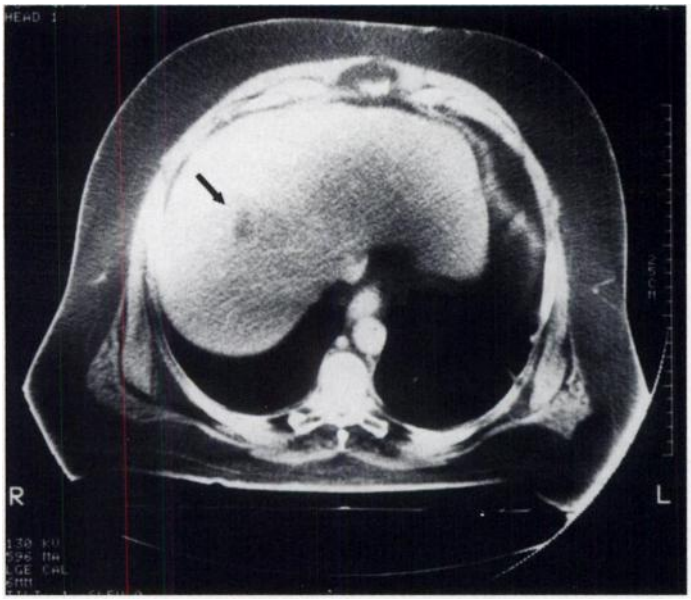

FIGURE 2. Contrast-enhanced CT performed several days after initial CT shows the hepatic abscess within the right hepatic lobe to be more mature and focal. No other hepatic abnormalities are present.

DISCUSSION

Our case demonstrates that a photopenic defect with a surrounding rim of increased activity within the hepatic parenchyma correlates with hepatic abscess. To our knowledge, this phenomenon has not been previously described with bacterial hepatic abscess. Remedios et al. described cholescintigraphic rim enhancement surrounding a photopenic region in 9 of 17 patients with amebic hepatic abscess (*1*). He suggests that this sign is specific for amebic hepatic abscess because hepatic lesions of other etiology did not reveal similar findings (*1*).

Pericholecystic hepatic uptake of radionuclide is a useful secondary sign in the cholescintigraphic diagnosis of acute cholecystitis (*2–4*). Proposed pathogenic mechanisms of development of the rim sign include hyperperfusion, as well as impaired radiopharmaceutical clearance. The latter mechanism is secondary to both hepatocyte dysfunction, with impaired excretion of radiopharmaceutical, and to edema of bile canniculi, with resultant bile stasis (*5–7*).

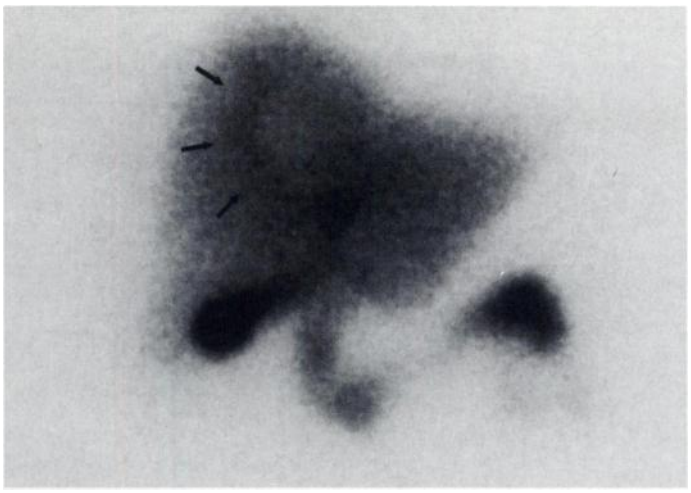

FIGURE 3. Anterior abdominal hepatobiliary image shows a rim of mildly prominent activity within the parenchyma of the right hepatic lobe surrounding a focus of diminished activity; the hepatic abscess rim sign.

CONCLUSION

The mechanisms of increased rim sign in cases of inflammation associated with adjacent gallbladder disease can be applied to the inflammatory changes seen in hepatic abscess. Inflammation leads to hyperemia, impairment of radiopharmaceutical excretion and a rim of increased activity.

The presence of a rim sign of increased activity surrounding an intrahepatic cold defect on hepatobiliary scan should lead to a high index of suspicion for hepatic abscess.

REFERENCES

1. Remedios PA, Colletti PM, Ralls PW. Hepatic amebic abscess: cholescintigraphic rim enhancement. *Radiology* 1986;160:395–398.
2. Swane LC, Ginsberg HN. Diagnosis of acute cholecystitis by cholescintigraphy: significance of pericholecystic hepatic uptake. *Am J Roentgenol* 1989;152:1211–1213.
3. Lowry PA, Tran HD. Delayed visualization of the gallbladder with a rim sign. *Clin Nucl Med* 1991;16:1–3.
4. Smith R, Rosen JM, Gallo LN, et al. Pericholecystic hepatic activity in cholescintigraphy. *Radiology* 1985;156:797–800.
5. Meekin GK, Ziessman HA, Klappenbach RS. Prognostic value and pathophysiologic significance of the rim sign in cholescintigraphy. *J Nucl Med* 1987;28:1679–1682.
6. Bushnell DL, Perlman SB, Wilson MA, et al. The rim sign: association with acute cholecystitis. *J Nucl Med* 1986;27:353–356.
7. Morrison RC, Ramos-Gabatin A, Gelormini RG, et al. Prompt visualization of the gallbladder with a rim sign: acute or subacute cholecystitis? *J Nucl Med* 1993;34:1169–1171.

Leukocyte-Marrow Scintigraphy in Hyperostosis Frontalis Interna

Maria Aurora Torres and Christopher J. Palestro
Division of Nuclear Medicine, Long Island Jewish Medical Center, New Hyde Park, New York

Hyperostosis frontalis interna is the term used to describe the thickening of the frontal bones of the skull. This thickening of the frontal bones is accompanied by an increase in the diploic space which results in an increased quantity of hematopoietically active marrow. Increased frontal bone uptake of labeled leukocytes has been reported in this condition, and the symmetric appearance of this activity may suggest its benign etiology. We have encountered a case of hyperostosis frontalis interna in which the uptake of labeled leukocytes was asymmetric and marrow scintigraphy confirmed that the activity seen was due to marrow not infection.

Key Words: hyperostosis frontalis interna; skull; marrow scintigraphy

J Nucl Med 1997; 38:1283–1285

Received Nov. 13, 1996; accepted Dec. 23, 1996.

For correspondence or reprints contact: Christopher J. Palestro, MD, Division of Nuclear Medicine, Long Island Jewish Medical Center, 270-05 76th Ave., New Hyde Park, NY 11040.

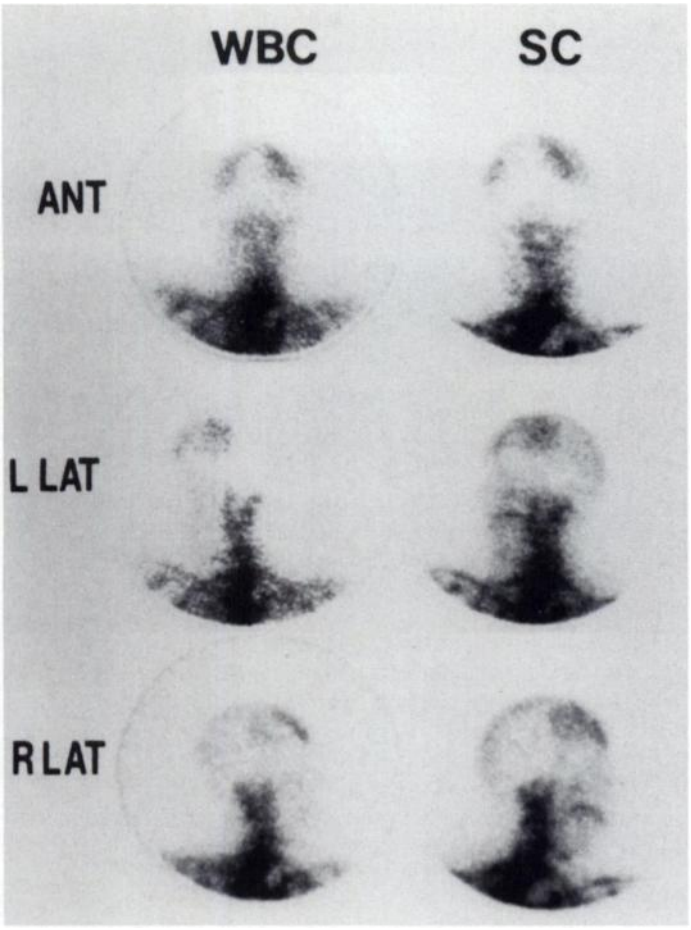

FIGURE 1. Labeled leukocyte (WBC) and sulfur colloid (SC) marrow images of this 78-yr-old woman with HFI. The asymmetric distribution of activity in the frontal bones (left greater than right) is virtually identical in both studies, confirming that the activity on the WBC images is due to marrow, not infection.

Hyperostosis frontalis interna (HFI) is the term applied to thickening of the skull which is usually limited to the squamous portion of the frontal bone, and affects particularly the subdural surface of the bone. Increased activity on labeled leukocyte imaging has been reported in this condition (*1,2*), and it has been suggested that the symmetric appearance of such increased activity may be useful for distinguishing HFI from infection. We have encountered a case of HFI in which the distribution of labeled leukocyte activity in the calvarium was asymmetric, and complimentary marrow scintigraphy provided useful information.

CASE REPORT

A 78-yr-old woman with a history of hypertension, chronic obstructive pulmonary disease and asthma was admitted to our institution for depression. During her admission, she developed a fever to 39°C, and underwent ^{111}In-labeled leukocyte scintigraphy as part of the diagnostic workup. Imaging was performed ~24 hr after injection of ~18.5 MBq of mixed autologous leukocytes labeled with ^{111}In according to the method of Thakur et al. (*3*). Six-minute images were acquired on a large field of view gamma camera equipped with a medium-energy collimator. Energy discrimination was accomplished using 15% windows centered around the 174 and 247 keV photopeaks of ^{111}In. The only abnormality observed on the labeled leukocyte study was asymmetric uptake of labeled cells in the frontal bones of the skull, which was greater on the left than on the right. Marrow scintigraphy was then performed to ascertain whether or not osteomyelitis was present. Approximately 1 hr after injection of 370 MBq ^{99m}Tc-sulfur colloid, 6 min anterior and lateral views of the skull were obtained using a low-energy, high-resolution collimator and a 10% window centered around the 140 keV photopeak of ^{99m}Tc. The distribution of activity on the marrow images was identical to that on the labeled leukocyte images, confirming that the findings on the leukocyte study were due to marrow, not osteomyelitis (Fig. 1). Subsequent radiographs demonstrated the presence of HFI in this patient (Fig. 2).

DISCUSSION

Hyperostosis frontalis interna is observed almost exclusively in women, and has been associated with various endocrine, metabolic and psychiatric disorders. The clinico-anatomic complex of calvarial thickening, virilism and obesity are often described as the "Morgagni" or "Stewart-Morel" syndrome. It has been postulated that the calvarial thickening which occurs

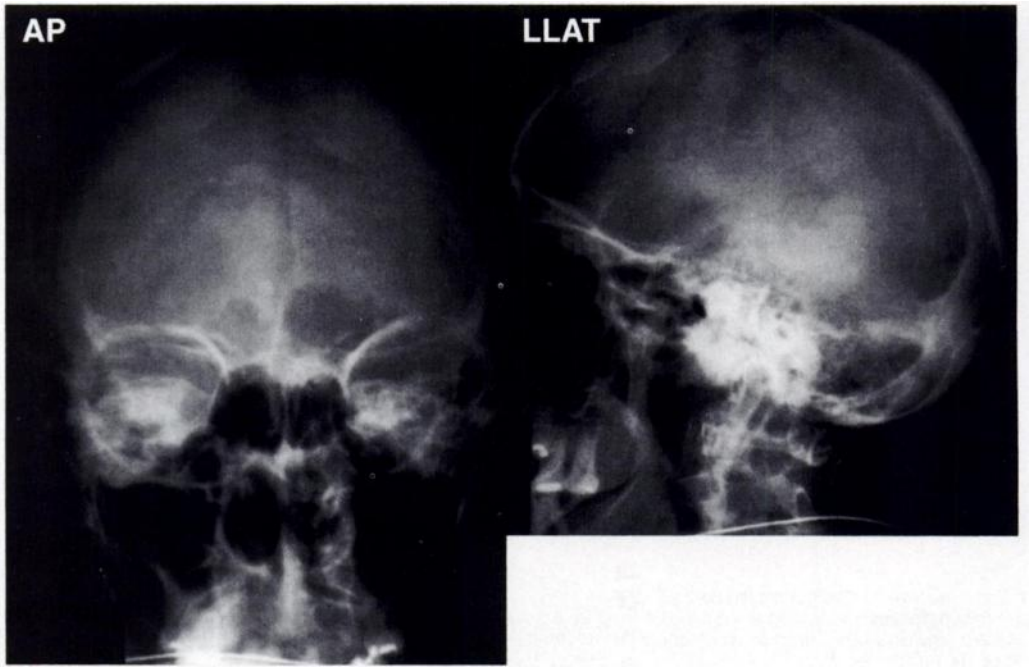

FIGURE 2. Anteroposterior and left lateral skull radiographs demonstrate the nodular, sclerotic, thickening of the inner table of the frontal bones with sparing of the outer table, characteristic findings in hyperostosis frontalis interna. The radiographic changes, in contrast to the radionuclide changes, are symmetric in appearance.

in HFI causes displacement of the brain which in turn strains the pituitary stalk resulting in the various endocrine manifestations of this syndrome (*4*).

The pathogenesis of this condition serves to explain the findings on the labeled leukocyte study. The frontal bones of the skull, along with most of the remainder of the calvarium, are comprised of two layers of compact bone known as the inner and outer tables. These two tables are separated from each other by the diploe, the cancellous bone containing hematopoietically active marrow within its interstices (*5*). The calvarial thickening of HFI is generally confined to the squamous portion of the frontal bones of the skull, and results from new bone deposition by the dura on the inner table. As the dura deposits new bone along the interior border of the inner table, the inner table itself undergoes spongification on its diploic side, resulting in excessive diploic bone in the thickened part of the calvarium (*4*). This increased diploic space is accompanied by a similar increase in the quantity of marrow, and it is this increased volume of marrow that undoubtedly accounts for the increased activity observed on labeled white cell images. The symmetric appearance of such increased calvarial activity is useful for distinguishing HFI from infection (*1,2*). Not all cases of HFI are symmetric, however, as this case illustrates, and in this situation determining the cause of the increased activity, is more problematic. Under these conditions, marrow scintigraphy can provide useful information. If the leukocyte and marrow images are spatially congruent, the findings on the labeled leukocyte study can be attributed to the increased marrow volume associated with HFI; if there is no activity on the marrow images corresponding to that on the leukocyte study, then the findings on the leukocyte study are due to infection (*6,7*).

CONCLUSION

Increased frontal bone activity on labeled leukocyte images of patients with HFI is due to the increased volume of marrow present in this condition; when doubts about the etiology of this increased uptake arise, adjunctive marrow imaging can provide useful information.

REFERENCES

1. Floyd JL, Jackson DE Jr, Carretta R. Appearance of hyperostosis frontalis interna on indium-111-leukocyte scans: potential diagnostic pitfall. *J Nucl Med* 1986;27:495–497.
2. Paulson E, Datz FL. False-positive calvarial uptake of indium-111 leukocytes in a patient with hyperostosis frontalis interna. *Clin Nucl Med* 1988;13:68–69.
3. Thakur ML, Lavender JP, Arnot RN, Silvester DJ, Segal AW. Indium-111-labeled autologous leukocytes in man. *J Nucl Med* 1977;18:1014–1021.
4. Various Hyperostoses of Obscure Origin. In: Jaffe HL, ed. *Metabolic, degenerative and inflammatory diseases of bones and joints*. Philadelphia: Lea and Febiger; 1972:272–300.
5. Osteology. In: Warwick R, Williams PL, eds. *Grays anatomy*, 35th ed., Edinburg, Longman; 1973:200–387.
6. Palestro CJ, Kim CK, Swyer AJ, Capozzi JD, Solomon RW, Goldsmith SJ. Total hip arthroplasty: periprosthetic ^{111}In-labeled leukocyte activity and complementary ^{99m}Tc sulfur colloid imaging in suspected infection. *J Nucl Med* 1990;31:1950–1955.
7. Palestro CJ, Roumanas P, Kim CK, Goldsmith SJ. Diagnosis of musculoskeletal infection using combined ^{111}In-labeled leukocyte and ^{99m}Tc-sulfur colloid marrow imaging. *Clin Nucl Med* 1992;17:269–273.

Compartmental Analysis of the Complete Dynamic Scan Data for Scintigraphic Determination of Effective Renal Plasma Flow

M.S. Dagli, V.J. Caride, S. Carpenter and I.G. Zubal

Division of Imaging Science, Department of Diagnostic Radiology, Yale Medical School, New Haven, Connecticut; and Section of Nuclear Medicine, Department of Radiology, The Hospital of Saint Raphael, New Haven, Connecticut

We have developed an image-based compartmental analysis for estimating effective renal plasma flow (ERPF in units of milliliters per minute) from the full time-activity curves of regions of interest (ROI) placed over the heart, kidneys and bladder. **Methods:** Kidney or time-activity curves are corrected for physical attenuation using estimates of kidney depth derived from patient height and weight. Estimates of the calibration factors, K_p and K_b (mCi/counts/sec), for the plasma and bladder time-activity curves are determined by applying the following ROI analysis to each frame of the dynamic scan: $(K_p)P_c(t) + (K_b)B_c(t) = D_i - R_q(t)$, where $P_c(t)$ and $B_c(t)$ represent the counting rates measured in ROI placed over the left ventricle blood pool and bladder at time t; D_i is the known total injected dose, and $R_q(t)$ represents the millicurie of tracer in the kidneys at time t. Once K_p and K_b have been determined by regression, the calibrated time activity curves are used to solve for the physiological parameter fERPF (min^{-1}), which represents the fraction of the total body plasma cleared of mertiatide per min. The ERPF calculated by the product of fERPF and plasma volume, determined from patient weight, was compared to the ERPF as calculated by blood samples and the Schlegel and renal uptake plasma volume product scintigraphic techniques. **Results:** Twenty-five adult patients with a wide range of ages and renal function were studied. The results of this image-based method for calculating ERPF correlated well with the values obtained from blood samples (linear regression slope = 1.06; y-int = −34.68 ml/min, r = 0.905) and offered a significant improvement over both the Schlegel and renal uptake plasma volume product estimates ($p < 0.05$). **Conclusion:** A scintigraphic estimation of ERPF without blood samples using time-activity data from the heart, kidneys and bladder acquired over the entire renogram is feasible and correlates well with more invasive techniques requiring blood samples.

Key Words: renal scintigraphy; technetium-99m-mertiatide; effective renal plasma flow; compartmental model

J Nucl Med 1997; 38:1285–1290

The accurate purely scintigraphic estimation of renal function has long been a goal in clinical nuclear medicine. Current clinically useful measurements of effective renal plasma flow (ERPF) require one or two blood samples for the processing of

Received Mar. 22, 1996; revision accepted Oct. 8, 1996.

For correspondence or reprints contact: George Zubal, PhD, Yale University School of Medicine, P.O. Box 208042, New Haven, CT 06520-8042.